GEOPHYSICS, VOL. 73, NO. 3 (MAY-JUNE 2008); P. F97–F104, 6 FIGS.
10.1190/1.2898410

Shaping optimal transmitter waveforms for marine CSEM surveys

Rune Mittet[1] and Tor Schaug-Pettersen[1]

ABSTRACT

The square wave is frequently used as the transmitter waveform in marine controlled-source electromagnetics (CSEM) surveys. This waveform has the advantage of transferring maximum energy to the subsurface because the transmitter current is running at its peak amplitude at all times. However, a limitation of the square wave is that most of the transmitted energy is in the first harmonic. Processing methods such as depth migration and inversion have shown improved results if a transmitter waveform with substantial amounts of energy at multiple frequencies is used. We propose a method for designing transmitter waveforms where current amplitudes as a function of frequency can have an approximate predefined or desired distribution. At the same time, we require that the transmitter operate at its peak current at all times to maximize the energy transferred to the subsurface. To obtain the desired current spectra, the number of switching times in a period is allowed to be larger than two, which is the number of switching times per period for a standard square wave. The method is based on matching the desired frequency spectra with the spectra obtained from these generalized square waves. This optimization problem is solved by a Monte Carlo method. The resultant waveforms can be used for an electric-dipole transmitter.

INTRODUCTION

Marine controlled-source electromagnetics (CSEM), or seabed logging (SBL), is an established technique for hydrocarbon exploration (Eidesmo et al., 2002; Ellingsrud et al., 2002; Srnka et al., 2006). Marine CSEM methods use an electric dipole to probe the subsurface. The technique has proven particularly useful for detecting thin, highly resistive layers that are typical for hydrocarbon reservoirs.

The square wave is frequently used as the transmitter waveform. This type of waveform is easy to generate. The electric-dipole transmitter runs maximum current at one polarity for half a period. The polarity is then switched for the second half of the period. The square wave has the advantage of transferring maximum energy to the subsurface because the source current is running at its peak value at all times except for possible switching intervals. The frequency-domain current amplitudes of the square wave are proportional to the inverse of the frequency, so the current amplitudes are reduced with increased frequency. At the same time, the absorption of the EM field increases with frequency.

Processing methods such as depth migration and inversion improve results if the recorded data have multiple frequencies with substantial energy. Thus, it can be desirable to partially counteract the offset-dependent increased loss of field strength with frequency by distributing more power to higher frequencies in the transmitter waveform than is possible with the square wave.

There can be situations where survey planning indicates the standard square is the best choice. On the other hand, survey planning might also indicate a better result can be obtained with a transmitter waveform having a frequency spectrum that differs from the standard square wave spectrum. Introducing such waveforms will increase experimental flexibility.

The idea of modifying the frequency spectrum of the standard square-wave transmitter signal is not new. Constable and Cox (1996) proposed a waveform that distributed the main energy contributions equally on the first and third harmonics. This can be obtained by switching the transmitter current more than twice per period. The amplitudes of these two spectral components are approximately 79% of the time-domain maximum current. For part of each period, no current is running. This reduces the total output from the transmitter. Lu and Srnka (2005) propose several waveforms with more than two switching times in one period. One of these waveforms has a spectrum where the main energy contributions are shared equally between the first, second, and fourth harmonics. The amplitudes of these three spectral components are approximately 61% of the time-domain maximum current. This assumes the current can be switched instantaneously from one polarity to the other.

A second waveform has a spectrum where the main energy contributions are shared equally between the first, second, fourth, and eighth harmonics. The amplitudes of these four spectral components are approximately 60% of the time-domain maximum current.

Manuscript received by the Editor 2 April 2007; revised manuscript received 2 September 2007; published online 10 April 2008.
[1]EMGS AS, Trondheim, Norway. E-mail: rm@emgs.com; tsp@emgs.com.

Again, this assumes the transmitter current can be switched instantaneously from one polarity to the other. If this is not the case, then the higher frequencies will suffer a somewhat reduced amplitude, depending on the length of the finite switching interval with zero current running in the transmitter. Both the Constable-Cox and the Lu-Srnka waveforms have substantial current amplitude at the desired frequencies and have seen practical use in marine CSEM surveys.

The damping of the EM field is very strong in marine CSEM surveys. It is advantageous to distribute the source energy to a limited number of frequencies for a towed transmitter system. This ensures that at these frequencies the EM field has the potential to propagate to receivers at large offset yet have amplitudes above the noise floor of the recording system.

A more continuous frequency spectrum can be obtained by transmitting a pseudorandom binary sequence (PRBS) as proposed by Duncan et al. (1980). The current amplitude for each frequency is significantly smaller for a PRBS signal than for the target frequencies of the generalized square waves described above. To increase the signal-to-noise ratio, repeated experiments should be performed at each source location (Helwig et al., 1999). This can be achieved by keeping the source stationary for multiple source runs before moving to a new location. This will have some impact on the operational efficiency of a marine survey because there is reduced subsurface coverage over a given time period compared to a towed electric-dipole system.

We propose a generalized square wave that combines maximum power with a desired frequency spectrum. The advantage is that more than a few frequencies with appreciable amplitude can be acquired in a single tow line. The maximum power is obtained by having an active source at maximum negative or positive current at all times. The method is based on the assumption that there can be a short period of zero current in the transmitter when switching from a negative to a positive current direction or vice versa. This is typical for a thyristor-based transmitter where the wait time is approximately 80 ms. This switching interval is much smaller for a transistor-based transmitter, possibly less than 5 ms. Our method covers both of these cases and the situation where the zero-current switching interval can be neglected.

Constable and Cox (1996) explain their choice of waveform by stating that transmitting multiple frequencies with equal amplitude can improve the ability to discriminate the signal from spurious effects. Lu and Srnka (2005) point our that multiple source frequencies at uniformly high power are highly desirable so that a range of depths can be probed using only one source tow. It is our experience that several advanced processing schemes, such as depth migration and inversion (Mittet et al., 2004; Mittet et al., 2005; Mittet et al., 2007), improve results because an increased number of frequencies can penetrate to moderate and large depths. With a standard square wave, this can be achieved by towing the same line several times with different base frequencies. As mentioned by Lu and Srnka, there is a potential cost reduction if a richer frequency spectrum can be obtained from a single towline.

In our opinion, it is unnecessary for the large-amplitude spectral components of the transmitter current to be of equal size. The important issue is to keep the EM field above the noise floor of the recording system to a high offset for the target frequencies. For any of these frequencies, this will also maximize the depth of investigation. Electromagnetic field amplitudes at different frequencies can be compared in a systematic way after normalization with the transmitter dipole moment as long as the EM field is maintained above the noise floor.

THEORY

We consider a periodic waveform for the transmitter current, where the current is allowed to switch polarity M times during a period. For the standard square wave, the transmitter current switches sign twice during a period, so we allow M to be equal to or larger than two. We can consider M to be an even integer because we work with a periodic signal. The transmitter current $J(t)$ is assumed to be periodic with a period T_0:

$$J(t) = J(t + T_0). \tag{1}$$

The transmitter current can be represented by the following Fourier series,

$$J(t) = \sum_{n=-\infty}^{\infty} \tilde{J}_n e^{-i\omega_n t}, \tag{2}$$

with Fourier coefficients

$$\tilde{J}_n = \frac{1}{T_0}\int_0^{T_0} dt J(t) e^{i\omega_n t}. \tag{3}$$

The angular frequency ω_n is

$$\omega_n = n\omega_0, \tag{4}$$

with

$$\omega_0 = 2\pi f_0 = 2\pi \frac{1}{T_0}. \tag{5}$$

However, because the transmitter waveform is real, we have

$$\tilde{J}_{-n} = \tilde{J}_n^*. \tag{6}$$

By using $J_n = 2\tilde{J}_n$,

$$J(t) = \frac{1}{2}J_0 + \sum_{n=1}^{\infty} \mathrm{Re}(J_n e^{-i\omega_n t}), \tag{7}$$

and we obtain the spectral current amplitudes

$$J_n = \frac{2}{T_0}\int_0^{T_0} dt J(t) e^{i\omega_n t}. \tag{8}$$

With this convention, we observe that the Fourier coefficients J_n have the same unit as $J(t)$. Note also that if $J(t)$ is a harmonic waveform with peak amplitude $J_{\max}$ in amperes and angular frequency ω_k, that is,

$$J(t) = J_{\max}\cos(\omega_k t), \tag{9}$$

then the spectral component at angular frequency ω_k equals the maximum current amplitude:

$$J_k = J_{\max}. \tag{10}$$

We split a period into a time-ordered sequence S_M of $M + 1$ times,

$$S_M = \{t_0, \ldots, t_{m-1}, t_m, t_{m+1}, \ldots, t_M\}, \tag{11}$$

such that $t_0 = 0$ and $t_M = T_0$. We assume that time t_0 belongs to the previous period. The times t_m in this sequence are then switching times at which the direction of the current changes 180° with respect to the transmitter orientation. The current amplitude is assumed to be at the peak value between switching times.

In the derivation to follow, we choose the current to be at the positive peak value on the first interval from t_0 to t_1. Let $J_{\max}$ be the maximum current for the transmitter; then the proposed transmitter waveform can be written

$$J(t) = (-1)^{m-1} J_{\max} \quad t_{m-1} < t \le t_m. \tag{12}$$

Equation 12 must be modified slightly if a thyristor-based transmitter is analyzed. The reason is that such a transmitter cannot switch instantaneously between positive and negative current directions at full load. It will have a switching interval t_s that is approximately 80 ms. In this interval, the current is zero. We can include this effect by modifying equation 12. Let t_σ be half the switching interval,

$$t_s = 2t_\sigma. \tag{13}$$

Then the transmitter time function, including the effect of a finite switching interval, is

$$J(t) = 0 \quad t_{m-1} < t \le t_{m-1} + t_\sigma,$$

$$J(t) = (-1)^{m-1} J_{\max} \quad t_{m-1} + t_\sigma < t \le t_m - t_\sigma,$$

and

$$J(t) = 0 \quad t_m - t_\sigma < t \le t_m. \tag{14}$$

The Fourier representation for the part of the transmitter current that is defined on the interval m is

$$J_n(m) = J_{\max} \frac{2}{T_0} (-1)^{m-1} \int_{t_{m-1}+t_\sigma}^{t_m - t_\sigma} dt e^{i\omega_n t}. \tag{15}$$

The integral gives

$$J_n(m) = J_{\max} \frac{2}{n\pi} (-1)^{m-1} e^{i\omega_n \tau_m} \sin[\omega_n(\Delta t_m - t_\sigma)], \tag{16}$$

where

$$\tau_m = \frac{1}{2}(t_m + t_{m-1})$$

and

$$\Delta t_m = \frac{1}{2}(t_m - t_{m-1}). \tag{17}$$

The contribution from all intervals must be summed,

$$J_n = \sum_{m=1}^{M} J_n(m), \tag{18}$$

which with equation 16 gives

$$J_n = J_{\max} \frac{2}{n\pi} \sum_{m=1}^{M} (-1)^{m-1} e^{i\omega_n \tau_m} \sin[\omega_n(\Delta t_m - t_\sigma)]. \tag{19}$$

Parseval's theorem gives

$$\frac{1}{4} J_0^2 + \frac{1}{2} \sum_{n=1}^{\infty} |J_n|^2 = \frac{1}{T_0} \int_0^{T_0} dt |J(t)|^2, \tag{20}$$

which shows that the sum of squared spectral amplitudes is at a maximum when the current is at the peak value at all times during a period. For a current waveform that is not at the peak value at all times during a period, we have

$$\frac{1}{2} \sum_{n=1}^{\infty} \left| \frac{J_n}{J_{\max}} \right|^2 \le 1, \tag{21}$$

if it is assumed that the waveform gives no direct current contribution.

The optimization procedure can be made independent of the magnitude of the peak current by dividing both sides of equation 19 by $J_{\max}$ such that

$$J_n \to \frac{J_n}{J_{\max}} = \frac{2}{n\pi} \sum_{m=1}^{M} (-1)^{m-1} e^{i\omega_n \tau_m} \sin[\omega_n(\Delta t_m - t_\sigma)]. \tag{22}$$

Equation 22 is our forward model for calculating the spectrum resulting from a given switching time sequence S_M. However, in the examples to follow, we use a peak current of 1000 A when we plot results. This gives us a good idea of what we can expect in terms of spectral current amplitudes from a real transmitter system.

The spectrum of the standard square wave can be obtained by using $M = 2$ and $t_s = 0$ in equation 19:

$$|J_n| = J_{\max} \frac{4}{n\pi} \left[\frac{1}{2}(1 - (-1)^n) \right]. \tag{23}$$

This is a well-known expression. Only the odd harmonics contribute to the signal, and the amplitude of the first harmonic is a factor $4/\pi$ higher than the transmitter maximum current. A realistic square wave must include the effect of the switching intervals:

$$|J_n| = J_{\max} \frac{4}{n\pi} \left[\frac{1}{2}(1 - (-1)^n) \right] \left| \sin\left[\omega_n \frac{1}{4}(T_0 - 2t_s) \right] \right|. \tag{24}$$

Equipped with a forward model (equation 22) that calculates the frequency spectrum from the switching time sequence, the next step is to match the spectrum $|J_n|$ with a desired spectrum I_n. This is an optimization problem with the switching time sequence being the unknown. Equation 21 indicates that the normalized spectral value $|J_n|$ can never exceed $\sqrt{2}$. However, equation 21 is based on using a generalized square wave, in which case more than one frequency component different from zero must be present in the waveform spectrum. The actual upper limit for a single spectral component is found when there is a maximum in the correlation of the source waveform

with a harmonic component. If we assume that the normalized source time function is a Rademacher function with frequency ω_k,

$$J_{\text{norm}}(t) = \text{sign}(\sin(\omega_k t)), \tag{25}$$

we have

$$J_n = \frac{4}{\pi}\frac{k}{n}, \quad n \geq k, \tag{26}$$

which gives a maximum spectral component of $4/\pi$ for $n = k$.

To proceed, we define a desired current spectrum I_n, where I_n cannot exceed $4/\pi$. As an example, if we target the second, third, and fifth harmonics with equal amplitude at 70% of the maximum current of the transmitter, we can use

$$I_2 = 0.7,$$

$$I_3 = 0.7,$$

and

$$I_5 = 0.7. \tag{27}$$

All other values of I_n are set to zero. The spectrum $|J_n|$ will depend on the switching time sequence S_M. The problem at hand is to find S_M such that $|J_n|$ has a distribution of amplitudes as a function of harmonics that is as close to I_n as possible. One possible criterion is to minimize the least-squares error ε,

$$\varepsilon = \sum_{n=0}^{N} (|J_n| - I_n)^2. \tag{28}$$

The maximum frequency $f_{\max}$ used in the optimization determines the highest harmonic N to use in equation 28. We normally use a maximum frequency of 15 Hz because higher frequencies are hard to use in an SBL survey; accordingly,

$$N\omega_0 = 2\pi f_{\max}$$

and

$$N = T_0 f_{\max}. \tag{29}$$

At the outset, we do not know the optimum value of M. Equation 28 must be minimized for a range of M values starting with $M = 2$. The maximum value of M will vary with the complexity of the problem. However, there is clearly an upper limit to M when the switching interval t_s has a finite value. The total time the source is active during one period T_{Eff} can be written

$$T_{\text{Eff}} = T_0 - Mt_s. \tag{30}$$

We see that if $T_0 = 4$ s and $M = 10$, then $T_{\text{Eff}} = 3.2$ s for $t_s = 0.08$ s. Hence, in the case of a finite t_s, the power output is reduced when M increases.

It is possible to try to solve equation 28 with a local optimization scheme. However, we have chosen a global optimization scheme for this problem. Close inspection of equation 28 has revealed a multitude of local minima. The number of local minima increases with the number of switching times M, and we could not get a local optimization scheme to work properly for this problem.

The calculation of the spectral contributions $|J_n|$ is very fast, so a Monte Carlo simulation is possible. We then have a scheme that has the potential of avoiding local minima. The scheme is as follows: The outer loop is over M, which varies from two to 20, unless we find the smallest error for $M > 14$. In this case, the maximum value of M is increased further, and we make sure the smallest error is found for a value of M that is sufficiently small compared to the maximum value of M investigated. In our experience, a margin of six, as indicated here, is a good choice. For fixed M, we vary the elements of S_M using a random number generator. We calculate the error ε and compare it with previous values. We store S_M if the error is the smallest so far. For all values of M, we let the number of configurations tested increase with a factor proportional to M^2, using $M^2 \times 10^5$ iterations for $M = 2$. We get excellent results with fewer iterations but use a large margin because the computer time used to solve the problem is of no importance.

We can use several optimization criteria simultaneously and at no extra computing cost because we do a Monte Carlo simulation. For example, in parallel with estimating the time series that minimizes equation 28, we can estimate the time series that maximizes the correlation measure γ in

$$\gamma = \sum_{n=0}^{N} \sqrt{|J_n| I_n}. \tag{31}$$

For the same desired transmitter current spectrum, it might be that this criterion gives a slightly different result than the least-squares norm in equation 28. It is up to the end user to choose between the resulting waveforms.

Further constraints on the solution can be introduced in a straightforward manner. If a transmitter waveform with zero DC contribution is desired, then we reject all solutions with a DC contribution, that is, for $|J_0| > 0$. Similarly, we can reject solutions where the interval between two consecutive switching times t_{m-1} and t_m is less than some limit $\Delta t_{\max}$. Such a limit can be useful to include in the design and analysis of transmitter waveforms, especially if the switching from positive to negative current or vice versa is not instantaneous for a particular transmitter system.

The optimization scheme used here is a Monte Carlo method with a greedy descent (or ascent) algorithm. This is a brute force approach but can be afforded because of the low CPU cost for calculating the forward model. We use a random-number generator to generate the switching time sequence. The random numbers are from 0.0 to 1.0.

Assume that the number of switching times M equals four. We first create four random numbers: r_1, r_2, r_3, r_4. This gives the auxiliary switching time sequence S_4^{aux},

$$\begin{aligned} S_4^{\text{aux}} &= \{t_0, t_1, t_2, t_3, t_4\}, \\ t_0 &= 0.0, \\ t_1 &= r_1, \\ t_2 &= t_1 + r_2, \\ t_3 &= t_2 + r_3, \\ t_4 &= t_3 + r_4. \end{aligned} \tag{32}$$

This sequence must be normalized such that the period is T_0. This is obtained by multiplying each switching time in the sequence by a factor of T_0/t_4. The normalized switching time sequence S_4 so obtained can be used in equation 22 to calculate the current amplitude spectrum.

RESULTS

The length of the switching interval of an electric dipole depends on the underlying hardware used to perform the change from one polarity to the reversed polarity. Figure 1 demonstrates the effect of a finite switching interval for the standard square wave. The black curve in Figure 1a is the transmitter time-domain signal for an ideal square wave with a period of 4 s. The current is running at an absolute value of 1000 A. The spectrum is shown as the black curve in Figure 1b. The green curve in Figure 1a shows the transmitter time-domain signal for a square wave with a switching interval of 80 ms. The spectrum is shown as the green curve in Figure 1b. In Figure 1b, we observe that the effect of the finite switching intervals is small on the first harmonic, but we see some relative reduction of amplitude with increased frequency. This is an expected effect because there must be reduced current amplitudes in the spectrum caused by the finite switching interval.

Figure 2 shows a solution to a design problem where we require

$$I_1 = 0.7,$$
$$I_2 = 0.7,$$
$$I_4 = 0.7. \tag{33}$$

Figure 2a shows the transmitter time-domain signal for a generalized square wave with a period of 4 s running a 1000-A current. The best solution is found for $M = 4$. The spectrum is shown in Figure 2b. The black curves are for a waveform with zero switching interval. The green curves are for a waveform with a switching interval of 80 ms. When including the switching interval of 80 ms, we observe that the amplitude of the first harmonic is 84% of the maximum current. The corresponding numbers for the second and fourth harmonics are 71% and 61%. The spectrum of the derived waveform does not match the design criterion perfectly. An arbitrary spectrum cannot be obtained with the present method.

The limiting factor is that we seek a maximum transmitter output by constraining the current to run at its peak value at all times except for possible switching intervals. However, what we can obtain is large current amplitudes (more than 60% of the maximum current in the above example) on all target frequencies. The waveform shown in Figure 2 is one in a subset of waveforms with similar spectra. We have the possibility to search for slightly different waveforms by redefining the design criterion. For example, if the spectrum in Figure 2 gives a less-than-desired amplitude on the fourth harmonic, we can try

$$I_1 = 0.6,$$
$$I_2 = 0.7,$$

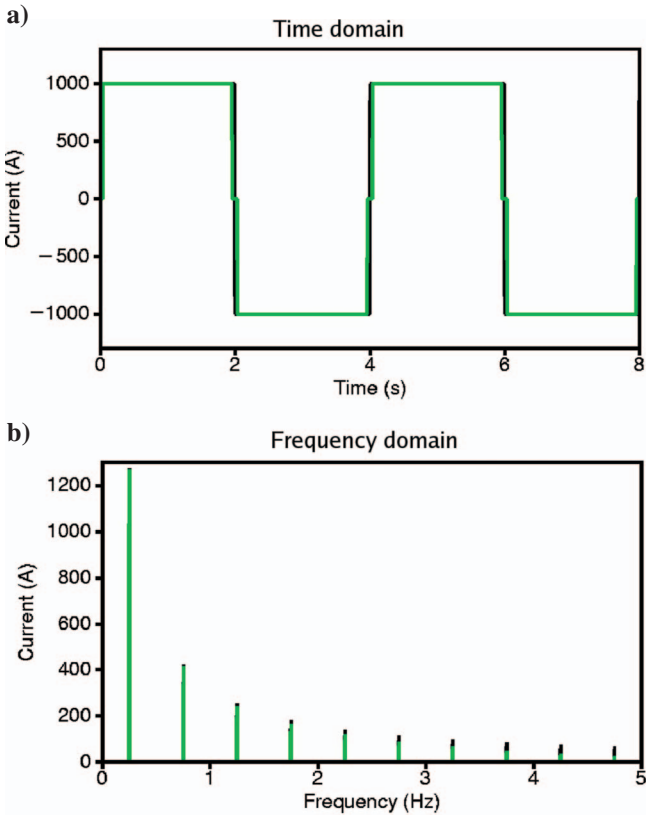

Figure 1. Standard square wave with a period of 4 s. The ideal square wave is shown in black. A square wave with a switching interval of 80 ms is shown in green. (a) Transmitter waveform; (b) current spectra.

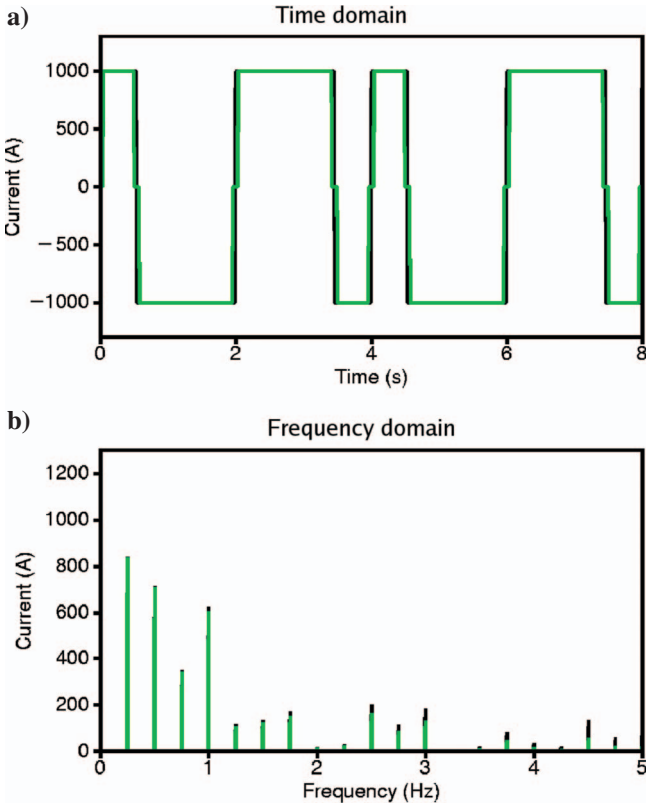

Figure 2. Generalized square wave with a period of 4 s. The optimization goal was to distribute currents to the first, second, and fourth harmonics. The generalized square wave with no switching interval is shown in black, and the generalized square wave with a switching interval of 80 ms is shown in green. (a) Transmitter waveform; (b) current spectra.

$$I_4 = 0.8. \tag{34}$$

The result is shown in Figure 3. Here, we obtain 59% on the first harmonic, 67% on the second harmonic, and 79% on the fourth harmonic.

The proposed method can also be used to generate broader frequency spectra. Figure 4 shows a solution to a design problem where we require

$$\begin{aligned} I_1 &= 0.6, \\ I_3 &= 0.6, \\ I_5 &= 0.6, \\ I_9 &= 0.6. \end{aligned} \tag{35}$$

Figure 4a shows the transmitter time-domain signal for a generalized square wave with a period of 4 s. The spectral components are shown in Figure 4b. The black curves are for a zero switching interval, and the green curves are for an 80-ms switching interval. For a negligible switching interval, we obtain 62% of the time-domain maximum current on the first harmonic, 67% on the third harmonic, 61% on the fifth harmonic, and 62% on the ninth harmonic. We observe a larger effect of a finite switching interval here than for the previous examples; but even with a finite switching interval, we have significant energy on the target frequencies. The first and third harmonics are not much affected. The fifth harmonic is down from 61% to 58%, and the ninth harmonic is down from 62% to 53% of the time-domain maximum current.

A real data example with the first harmonic at 0.25 Hz is shown in Figures 5 and 6. The black curve in Figure 5a is the result of the design problem,

$$\begin{aligned} I_1 &= 0.7, \\ I_3 &= 0.7, \\ I_5 &= 0.7. \end{aligned} \tag{36}$$

In other words, our target is 70% of the peak current at the first, third, and fifth harmonics. The green curve in Figure 5a is the measured current running in the transmitter. The differences from the designed current waveform are minor. The main effect not accounted for in our description of the transmitter system is the self-inductance of the antennae, which gives some deviation between the desired waveform and the real waveform at the switching times. The real waveform gives 71% at the first harmonic, 77% on the third harmonic, and 70% on the fifth harmonic.

Electric inline data from a receiver are shown in Figure 6. The spectral components are the first, third, fifth, seventh, ninth, and eleventh harmonics. The amplitudes of the inline electric field have the main contributions on the first, third, and fifth harmonics, as ex-

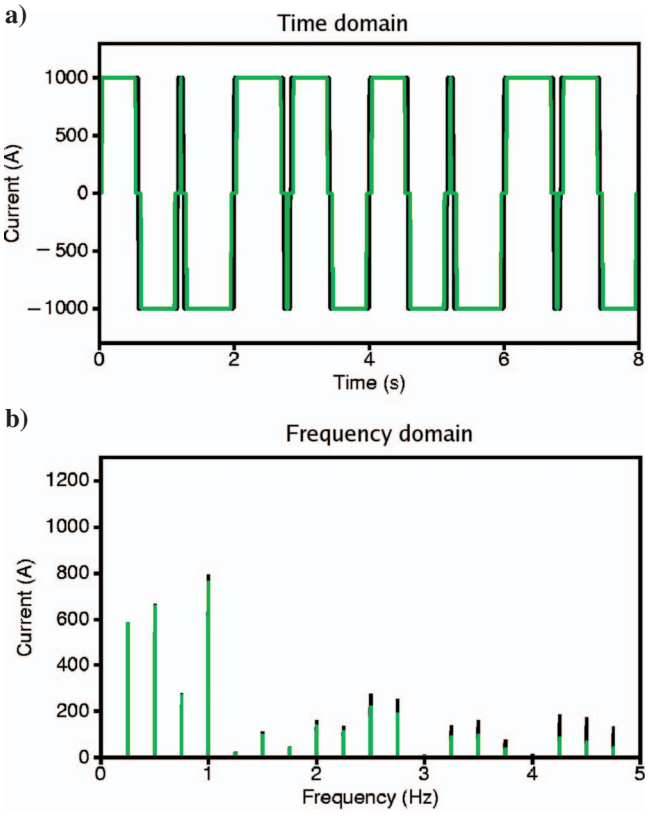

Figure 3. Generalized square wave with a period of 4 s. The optimization goal was to distribute currents to the first, second, and fourth harmonics with highest current amplitude on the fourth harmonic. The generalized square wave with no switching interval is shown in black, and the generalized square wave with a switching interval of 80 ms is shown in green. (a) Transmitter waveform; (b) current spectra.

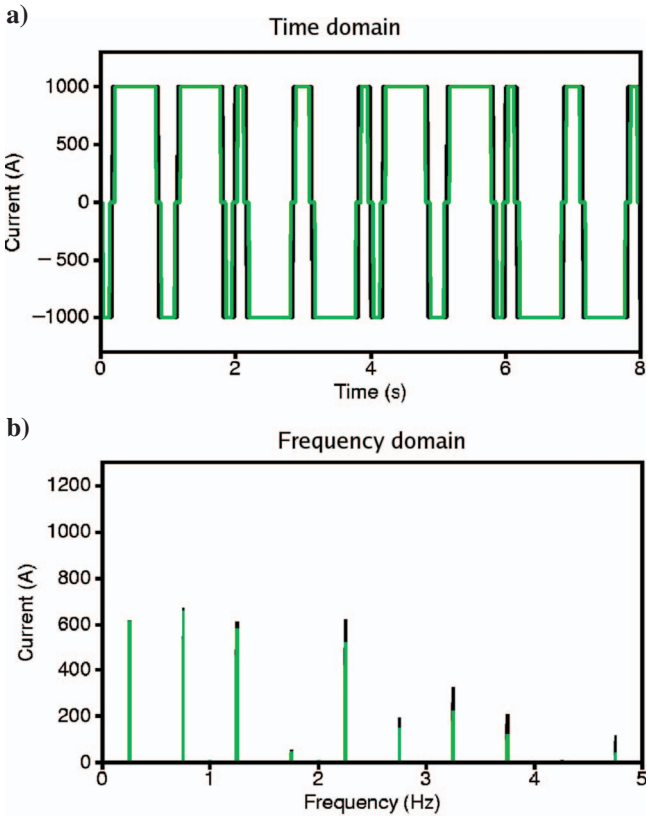

Figure 4. Generalized square wave with a period of 4 s. The optimization goal was to distribute currents to the first, third, fifth, and ninth harmonics. The generalized square wave with no switching interval is shown in black, and the generalized square wave with a switching interval of 80 ms is shown in green. (a) Transmitter waveform; (b) current spectra.

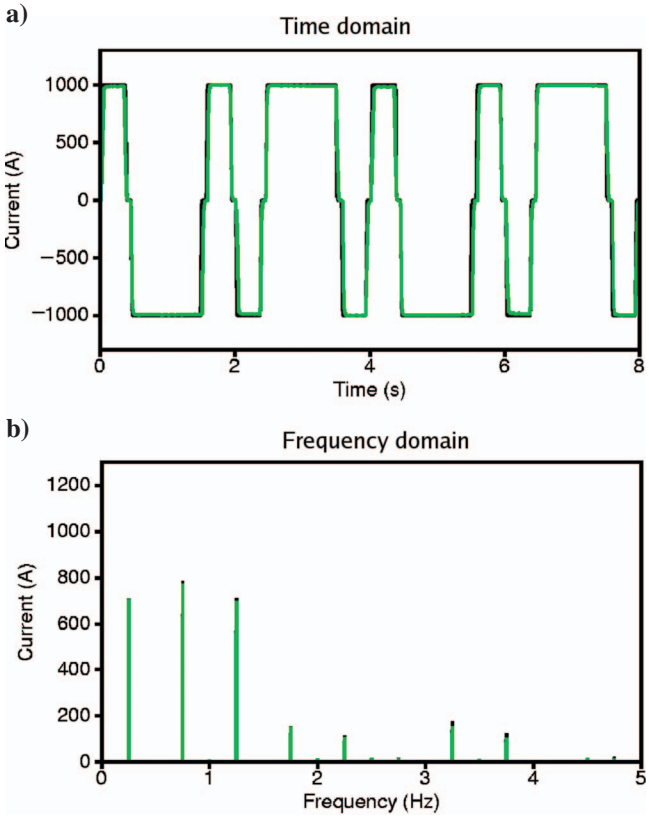

Figure 5. Generalized square wave with a period of 4 s. The optimization goal was to distribute currents to the first, third, and fifth harmonics. The designed generalized square wave with a switching time of 80 ms is shown in black. The current measured on the transmitter is shown in green. (a) Transmitter waveform; (b) current spectra.

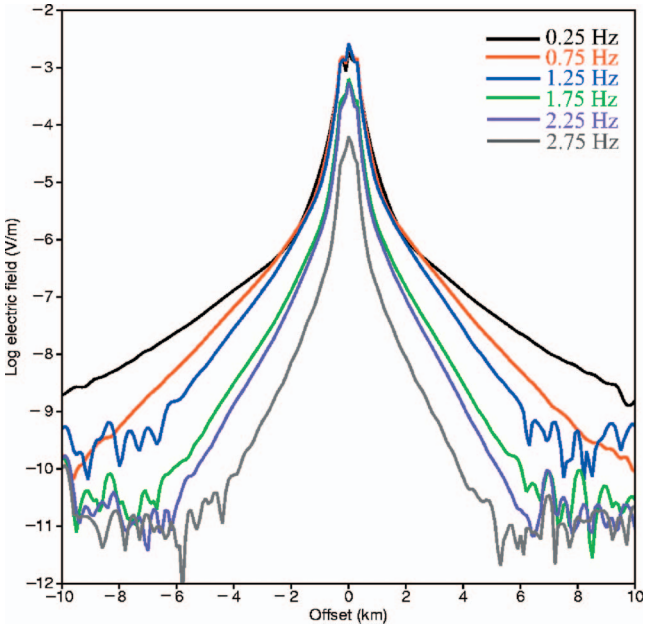

Figure 6. Measured inline electric field. The first six odd harmonics. Propagation losses are small at small offsets. The amplitudes at these offsets, as a function of frequency, follow the behavior of the transmitter current.

pected from the transmitted waveform. If we look at the data at very small offsets, where propagation losses are small, we observe that the amplitudes of the inline electric field have the same distribution as a function of frequency as the transmitter current. The first, third, and fifth harmonics are of equal amplitude. The seventh and ninth harmonics are also of equal amplitude but are smaller than the three target frequencies. Finally, the eleventh harmonic is nearly two orders of magnitude smaller than the target frequencies both in the transmitter current spectrum in Figure 5b and in the inline electric field spectrum in Figure 6.

A maximum offset of 10 km at 0.25 Hz is usually viewed as sufficient for hydrocarbon exploration. For 0.25 Hz, the inline electric field stays above the noise floor at all offsets for a transmitter current contribution of 710 A. The standard square wave at this frequency would give a transmitter current of 1273 A; however, 710 A is more than sufficient to stay above the noise floor. The waveform in Figure 5 has 770 A at 0.75 Hz. This is close to twice the value of the standard square wave amplitude at this frequency, which is 424 A. This frequency component stays above the noise floor for offsets up to at least 9 km. The 1.25-Hz current amplitude is 700 A. The standard square wave contributes 254 A at this frequency. This frequency component stays above the noise floor for offsets of up to approximately 6 km.

This line was not towed with a standard square wave, so a direct comparison is not possible. However, modeling results indicate that when the current amplitude is increased from 254 to 700 A there is an increase in the offset where the electric field stays above the noise floor. This increase in offset depends on subsurface resistivity, but for realistic assumptions it varies from 500 to 1000 m. The accompanying increase in depth of investigation ranges from 250 to 500 m.

CONCLUSION

We have introduced a method for generating transmitter waveforms with a desired current amplitude spectrum. A constraint is that we require that the transmitter operate at its peak current at all times to maximize the energy transferred to the subsurface. The effect of this constraint is that the fit between the desired spectrum and the spectrum derived for the optimal waveform can differ slightly. However, we can achieve our main goal, which is to obtain waveforms with high current amplitudes at the target frequencies. The optimal waveforms are derived by applying a Monte Carlo method.

Some transmitter systems cannot switch instantaneously between opposite polarities of the current. The effect of this finite switching interval is to reduce amplitudes at higher harmonics. Here, we have given one example for a broadband waveform with a period of 4 s where there is a 5% reduction on the fifth harmonic and a 15% reduction on the ninth harmonic. We have tested optimized waveforms in data acquisition and demonstrated that transmitted and recorded signals behave according to what we expect.

ACKNOWLEDGMENTS

We thank EMGS AS for allowing the publication of this work. We also thank three anonymous reviewers for very useful and constructive suggestions.

REFERENCES

Constable, S., and C. Cox, 1996, Marine controlled source electromagnetic sounding 2 — The PEGASUS experiment: Journal of Geophysical Research, **101**, 5519–5530.

Duncan, P. M., A. Hwang, R. N. Edwards, R. C. Bailey, and G. D. Garland, 1980, The development and applications of a wide band electromagnetic sounding system using a pseudo-noise source: Geophysics, **45**, 1276–1296.

Eidesmo, T., S. Ellingsrud, L. M. MacGregor, S. Constable, M. C. Sinha, S. Johansen, F. N. Kong, and H. Westerdahl, 2002, Sea bed logging (SBL), a new method for remote and direct identification of hydrocarbon filled layers in deepwater areas: First Break, **20**, 144–152.

Ellingsrud, S., T. Eidesmo, M. C. Sinha, L. M. MacGregor, and S. Constable, 2002, Remote sensing of hydrocarbon layers by seabed logging (SBL): Results from a cruise offshore Angola: The Leading Edge, **21**, 972–982.

Helwig, S. L., T. Hanstein, and A. Hördt, 1999, The VIBR OTEM method: 69th Annual International Meeting, SEG, Expanded Abstracts, 283–285.

Lu, X., and L. J. Srnka, 2005, Logarithmic spectrum transmitter waveform for controlled-source electromagnetic surveying: U. S. Patent WO 2005/117326A2.

Mittet, R., L. Løseth, and S. Ellingsrud, 2004, Inversion of SBL data acquired in shallow waters: 66th Annual Conference and Exhibition, EAGE, Extended Abstracts.

Mittet, R., F. A. Maaø, O. M. Aakervik, and S. Ellingsrud, 2005, A two-step approach to depth migration of low frequency electromagnetic data: 75th Annual International Meeting, SEG, Expanded Abstracts, 522–525.

Mittet, R., H. Maulana, K. Brauti, and T. A. Wicklund, 2007, CMP inversion of marine CSEM data: 69th Annual Conference and Exhibition, EAGE, Extended Abstracts.

Srnka, L. J., J. J. Carazzone, M. S. Ephron, and E. A. Eriksen, 2006, Remote reservoir resistivity mapping: The Leading Edge, **25**, 972–975.